ARMY RESEARCH LABORATORY

Analysis and Design of Resonant Charging System

Alan Bromborsky and Thomas Podlesak

ARL-TR-1819 December 1998

The findings in this report are not to be construed as an official Department of the Army position unless so designated by other authorized documents.

Citation of manufacturer's or trade names does not constitute an official endorsement or approval of the use thereof.

Destroy this report when it is no longer needed. Do not return it to the originator.

Army Research Laboratory

Adelphi, MD 20783-1197

ARL-TR-1819 **December 1998**

Analysis and Design of Resonant Charging System

Alan Bromborsky and Thomas Podlesak

Sensors and Electron Devices Directorate

Abstract

The circuit equations are constructed and solved for a simple resonant (single-pole) circuit and a dual-resonance (double-pole) capacitor charging system. Design equations are derived from the solutions. As an example, a command charging system for a capacitor is designed, with detailed equations given for the inductor and transformer analysis; an evaluation of suitable commercially available thyristors and capacitors is also provided.

Contents

Figures

Tables

1. Introduction

We present the analysis and design of a resonant charging system for the pulse-forming network (PFN) of a high-power microwave (HPM) system. The PFN charging system currently in use for the HPM system of interest uses an iron-core power transformer and weighs about 2000 lb. Our analysis shows that this charging system could be replaced with one that uses resonant charging with air-core inductors and transformers, reducing the weight of the PFN charging system to 350 lb. This change would enhance the Army's ability to field such systems on existing platforms. Further, although we designed the charging system with a particular HPM system in mind, the analysis and design techniques are applicable to generic HPM systems.

The major components of an HPM system are the prime power, the power-conditioning system, the microwave tube, and a load. The power-conditioning system itself usually consists of several stages of pulse compression and voltage and power amplification. Additionally, the power-conditioning system must present a compatible load impedance to the prime power system and an appropriate source impedance to the microwave tube. For short-pulse systems (<10 μs), the final stage of the power-conditioning system is generally a type-E Guillemin PFN [1, p 205] that is discharged through a pulse transformer. Because of the limitations of the voltage gain for this type of system, if several hundred kilovolts are required at the microwave tube, the capacitors in the PFN must be charged to several tens of kilovolts. For HPM systems that require portable prime power in the regime of 50 to 200 kW (a regime of interest in many directed-energy warfare scenarios), the power-conditioning system that forms the interface between the prime power (usually a diesel generator) and the modulator (PFN + pulse transformer) can easily be larger and heavier than the modulator if standard (even at 400 Hz) power transformation methods are used.

The parameter space for the HPM system of interest to us requires charging a capacitor (actually a PFN) to 42 kV with 250 J of energy and then discharging it in 2 μs, at a 300-Hz repetition rate. These specifications result in an average electrical power requirement of 75 kW (charging system out-

put power) to charge the capacitance of the PFN at the maximum 300-Hz repetition rate.

The first option that we explored to develop a charging power supply for the PFN was a switching power supply. The problem with this approach is that the load of the charging power supply is not resistive but capacitive (it has complex impedance). In order to maintain an average power flow of 75 kW to the capacitive load, the peak power rating of the power supply (constant current charging mode) has to be 150 kW. In switching power supplies, the size of the semiconductor switches is based on the peak power required. For our application, we would need a power supply that would cost on the order of $100 K, with no spare parts included. Additionally, we have had trouble in the field with systems that use switching power supplies because of uncontrollable environmental factors (the same power supplies work very well in the laboratory). Although we believe that the switching power supplies could be made to work well in the field, such a solution would entail an additional cost that we cannot currently afford.

As an alternative to switching power supplies, we explored command charging the PFN with a resonant charging system. The system would be optimized to charge a specific PFN at the maximum required repetition rate. Rather than using IGBTs (insulated gate bipolar transistors), the system would use thyristors for all switching (soft switching at zero current), providing reliable operation at reduced cost.

In the following, we analyze the two basic types of resonant charging of capacitors (simple inductive transfer and transformer-coupled transfer of energy), detail the properties of dual-resonance charging, and present a design exercise for a complete PFN charging system.

2. Analysis of Resonant Charging

2.1 Solution of Resonant Inductor Equations

The general inductor resonant charging circuit for a capacitance C_s is shown in figure 1. In this system, the usual condition is that the primary capacitor C_p is initially charged to a voltage V_0 and then discharged through the inductor. The capacitance connected to the output of the inductor, C_s, is initially uncharged.

The loop equation for the resonant inductor system in figure 1 is given by

$$V_0 - \frac{1}{C_p}\int_0^t i\ dt' = L\frac{di}{dt} + \frac{1}{C_s}\int_0^t i\ dt'. \tag{1}$$

Grouping terms gives

$$V_0 = L\frac{di}{dt} + \left(\frac{1}{C_p} + \frac{1}{C_s}\right)\int_0^t i\ dt'. \tag{2}$$

Define

$$\frac{1}{C} = \frac{1}{C_p} + \frac{1}{C_s} \tag{3}$$

and

$$\omega = \frac{1}{\sqrt{LC}}. \tag{4}$$

Then

$$\omega^2 C V_0 = \frac{di}{dt} + \omega^2 \int_0^t i\ dt'. \tag{5}$$

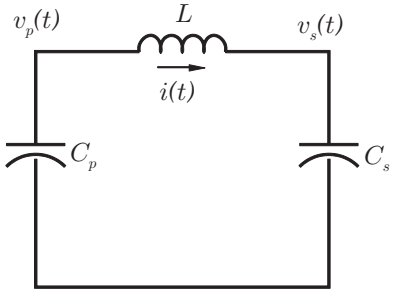

Figure 1. Resonant inductor capacitor charging circuit.

Now take the Laplace transform of equation (5) with the initial condition of $i(0) = 0$ and solve for $I(s)$:

$$\frac{\omega^2 C V_0}{s} = sI + \frac{\omega^2 I}{s}, \tag{6}$$

$$\frac{V_0}{L} = \left(s^2 + \omega^2\right) I, \tag{7}$$

$$I = \frac{1}{s^2 + \omega^2} \frac{V_0}{L}. \tag{8}$$

Taking the inverse Laplace transform of equation (8) [2, p 1022] gives

$$i(t) = \frac{V_0}{\omega L} \sin(\omega t). \tag{9}$$

The maximum values of i and di/dt are

$$\max\{i(t)\} = \frac{V_0}{\omega L} \quad \text{and} \tag{10}$$

$$\max\left\{\frac{di}{dt}\right\} = \frac{V_0}{L}. \tag{11}$$

The rms value is

$$\begin{aligned} \langle i \rangle_{rms} &= \sqrt{\mathcal{R} \int_0^{\frac{\pi}{\omega}} i^2 \, dt} \\ &= \frac{V_0}{\omega L} \sqrt{\frac{\mathcal{R}T}{2}}, \end{aligned} \tag{12}$$

where $\mathcal{R}$ is the repetition rate and T the charging time (one half cycle at frequency ω). The terms v_s and $\max\{v_s\}$ are calculated to be

$$\begin{aligned} v_s(t) &= \frac{1}{C_s} \int_0^t i \, dt' \\ &= \frac{V_0 C}{C_s} (1 - \cos(\omega t)) \quad \text{and} \end{aligned} \tag{13}$$

$$\max\{v_s(t)\} = \frac{2V_0 C}{C_s}. \tag{14}$$

The terms v_p and $\min\{v_p\}$ are

$$\begin{aligned} v_p(t) &= V_0 - \frac{1}{C_p}\int_0^t i\ dt' \\ &= V_0\left(1 - \frac{C}{C_p}(1-\cos(\omega t))\right), \end{aligned} \tag{15}$$

$$\min\{v_p(t)\} = V_0\left(1 - \frac{2C}{C_p}\right). \tag{16}$$

Although this circuit has a limiting maximum voltage gain of only two, it is still quite useful for the following characteristics:

1. The primary capacitor C_p is only partially discharged (see eq (15)). Where filtering of the system prime power (wall plug, generator, or battery) is required, the use of C_p for energy storage and filtering can be very advantageous.
2. A voltage gain of order two can be very useful if a much higher system voltage gain is needed that requires a transformer somewhere in the system. Use of a resonant inductor charging system can almost halve the turns ratio required by the transformer. This can lead to a significant size and weight reduction in the transformer.
3. Maximum energy transfer from C_p to C_s occurs when $i = 0$. This condition leads to simplified switching requirements.

In designing a resonant energy transfer circuit, one parameter that would probably be specified is the ratio of the energy $\mathcal{E}_p$ on capacitor C_p to maximum energy transferred $\mathcal{E}_s$ to capacitor C_s. This ratio is given by

$$\frac{\mathcal{E}_p}{\mathcal{E}_s} = \frac{C_p C_s}{4C^2}. \tag{17}$$

If $\mathcal{E}_p/\mathcal{E}_s$ is given and C_s or C_p is known, the unknown capacitance can be calculated from

$$\frac{C_s}{C_p} = \frac{\left(4\frac{\mathcal{E}_p}{\mathcal{E}_s} - 1\right) - \sqrt{\left(4\frac{\mathcal{E}_p}{\mathcal{E}_s} - 1\right)^2 - 4}}{2}. \tag{18}$$

Usually in designing a resonant energy transfer circuit as the first stage of power conditioning, one would specify the following parameters:

1. T, the time to charge C_s.

2. V_0, the voltage that C_p is initially charged to.
3. $\mathcal{E}_s$, the energy to be transferred to C_s.
4. $\mathcal{E}_p/\mathcal{E}_s$, the ratio of the energy stored on C_p to that transferred to C_s.

The design equations are then given by equation (18),

$$C_p = 2\left(\frac{\mathcal{E}_p}{\mathcal{E}_s}\right)\frac{\mathcal{E}_s}{V_0^2}, \quad \text{and} \tag{19}$$

$$L = \left(\frac{1}{C_p} + \frac{1}{C_s}\right)\left(\frac{T}{\pi}\right)^2. \tag{20}$$

2.2 Solution of Resonant Transformer Equations

The general transformer resonant charging circuit for a capacitance C_s is shown in figure 2. In this system, the usual condition is that the primary capacitor C_p is initially charged to a voltage V_0 and then discharged through the primary of the transformer. The capacitance across the secondary of the transformer, C_s, is initially uncharged.

The loop equations for the resonant transformer system in figure 2 are given by

$$V_0 = \frac{1}{C_p}\int_0^t i_p\, dt' + L_p\frac{di_p}{dt} + M\frac{di_s}{dt}, \tag{21}$$

$$0 = \frac{1}{C_s}\int_0^t i_s\, dt' + L_s\frac{di_s}{dt} + M\frac{di_p}{dt}. \tag{22}$$

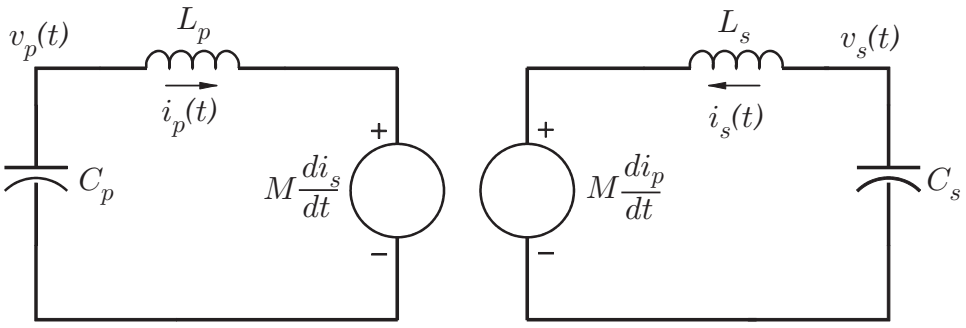

Figure 2. Resonant transformer capacitor charging circuit.

Multiplying equation (21) by C_p and equation (22) by C_s gives

$$C_p V_0 = \int_0^t i_p \, dt' + L_p C_p \frac{di_p}{dt} + M C_p \frac{di_s}{dt}, \tag{23}$$

$$0 = \int_0^t i_s \, dt' + L_s C_s \frac{di_s}{dt} + M C_s \frac{di_p}{dt}. \tag{24}$$

To simplify the system, define the primary and secondary resonant frequencies (ω_p and ω_s), the transformer coupling factor (k), and the generalized transformer turns ratio (N) by

$$\omega_p = \frac{1}{\sqrt{L_p C_p}}, \tag{25}$$

$$\omega_s = \frac{1}{\sqrt{L_s C_s}}, \tag{26}$$

$$k = \frac{M}{\sqrt{L_p L_s}}, \tag{27}$$

$$N = \sqrt{\frac{L_s}{L_p}}. \tag{28}$$

Substituting equations (25) through (28) into equations (23) and (24) gives

$$\omega_p^2 C_p V_0 = \omega_p^2 \int_0^t i_p \, dt' + \frac{di_p}{dt} + kN \frac{di_s}{dt}, \tag{29}$$

$$0 = \omega_s^2 \int_0^t i_s \, dt' + \frac{di_s}{dt} + \frac{k}{N} \frac{di_p}{dt}. \tag{30}$$

Laplace transforming $i_p(t)$ and $i_s(t)$ to $I_p(s)$ and $I_s(s)$ gives

$$\frac{\omega_p^2 C_p V_0}{s} = \frac{\omega_p^2 I_p}{s} + s I_p - i_p(0) + kN \left(s I_s - i_s(0) \right), \tag{31}$$

$$0 = \frac{\omega_s^2 I_s}{s} + s I_s - i_s(0) + \frac{k}{N} \left(s I_p - i_p(0) \right). \tag{32}$$

The initial conditions are $i_p(0) = 0$ and $i_s(0) = 0$, so that

$$\omega_p^2 C_p V_0 = \left(s^2 + \omega_p^2 \right) I_p + kN s^2 I_s, \tag{33}$$

$$0 = \left(s^2 + \omega_s^2 \right) I_s + \frac{k}{N} s^2 I_p, \tag{34}$$

$$I_s = -\frac{k}{N} \frac{s^2}{s^2 + \omega_s^2} I_p, \tag{35}$$

$$\omega_p^2 C_p V_0 = \frac{\left(s^2 + \omega_p^2 \right) \left(s^2 + \omega_s^2 \right) - k^2 s^4}{s^2 + \omega_s^2} I_p. \tag{36}$$

Define the resonant denominator for the system to be

$$\begin{aligned} D(s) &= \left(s^2+\omega_p^2\right)\left(s^2+\omega_s^2\right) - k^2 s^4 \\ &= \left(1-k^2\right)s^4 + \left(\omega_p^2+\omega_s^2\right)s^2 + \omega_p^2\omega_s^2. \end{aligned} \tag{37}$$

Now solve equations (35) and (36) for I_p and I_s:

$$I_p = \omega_p^2 C_p V_0 \frac{s^2+\omega_s^2}{D(s)}, \tag{38}$$

$$I_s = -\frac{k\omega_p^2 C_p V_0}{N}\frac{s^2}{D(s)}. \tag{39}$$

The denominator $D(s)$ can be factored into

$$\begin{aligned} D(s) &= \left(1-k^2\right)\left(s^2+\omega_+^2\right)\left(s^2+\omega_-^2\right) \\ &= \left(1-k^2\right)(s-i\omega_+)(s+i\omega_+)(s-i\omega_-)(s+i\omega_-), \end{aligned} \tag{40}$$

where the roots in equation (40) are given by

$$\boxed{\omega_\pm^2 = \frac{\omega_p^2+\omega_s^2 \pm \sqrt{\left(\omega_p^2+\omega_s^2\right)^2 - 4\left(1-k^2\right)\omega_p^2\omega_s^2}}{2\left(1-k^2\right)}.} \tag{41}$$

(Throughout the report, boxed equations are the critical design equations.)

Note that under no circumstances can $\omega_+ = \omega_-$, since this would require $\omega_p^2+\omega_s^2 = 2\sqrt{1-k^2}\omega_p\omega_s$, but $\omega_p^2+\omega_s^2 > 2\omega_p\omega_s > 2\sqrt{1-k^2}\omega_p\omega_s$. Since the Laplace transforms for the primary current I_p and secondary current I_s are the quotients of two polynomials with the denominator of higher degree than the numerator, and the denominator also has distinct roots (none repeat), the Laplace transforms can be inverted with the Heaviside expansion theorem [2, p 1021]. If $N(s)$ is the numerator and $D(s)$ is the denominator with

$$D(s) = (s-a_1)(s-a_2)\ldots(s-a_m), \tag{42}$$

then

$$\mathcal{L}^{-1}\left\{\frac{N(s)}{D(s)}\right\} = \sum_{n=1}^{m}\frac{N(a_n)}{D'(a_n)}e^{a_n t}. \tag{43}$$

For our system, the derivative of the denominator is

$$D'(s) = \left(1-k^2\right)\left(4s^3 + 2\left(\omega_+^2 + \omega_-^2\right)s\right), \tag{44}$$

and the values $D'(a_n)$ are

$$\begin{aligned}
D'(i\omega_+) &= -2i\left(1-k^2\right)\left(\omega_+^2 - \omega_-^2\right)\omega_+, & (45)\\
D'(-i\omega_+) &= 2i\left(1-k^2\right)\left(\omega_+^2 - \omega_-^2\right)\omega_+, & (46)\\
D'(i\omega_-) &= 2i\left(1-k^2\right)\left(\omega_+^2 - \omega_-^2\right)\omega_-, & (47)\\
D'(-i\omega_-) &= -2i\left(1-k^2\right)\left(\omega_+^2 - \omega_-^2\right)\omega_-. & (48)
\end{aligned}$$

The secondary current is

$$i_s(t) = -\frac{k\omega_p^2 C_p V_0}{N}\mathcal{L}^{-1}\left\{\frac{s^2}{D(s)}\right\}, \tag{49}$$

$$\mathcal{L}^{-1}\left\{\frac{s^2}{D(s)}\right\} = \frac{\omega_+\sin(\omega_+ t) - \omega_-\sin(\omega_- t)}{\left(1-k^2\right)\left(\omega_+^2 - \omega_-^2\right)}, \tag{50}$$

$$\boxed{i_s(t) = -\left(\frac{k\omega_p^2 C_p V_0}{N}\right)\frac{\omega_+\sin(\omega_+ t) - \omega_-\sin(\omega_- t)}{\left(1-k^2\right)\left(\omega_+^2 - \omega_-^2\right)}.} \tag{51}$$

The primary current is

$$i_p(t) = \omega_p^2 C_p V_0 \mathcal{L}^{-1}\left\{\frac{s^2+\omega_s^2}{D(s)}\right\}, \tag{52}$$

$$\begin{aligned}
\mathcal{L}^{-1}\left\{\frac{s^2+\omega_s^2}{D(s)}\right\} &= -\frac{1}{\left(1-k^2\right)\left(\omega_+^2 - \omega_-^2\right)} \\
&\quad \times\left\{\frac{\omega_s^2-\omega_+^2}{\omega_+}\sin(\omega_+ t) - \frac{\omega_s^2-\omega_-^2}{\omega_-}\sin(\omega_- t)\right\}, \quad (53)
\end{aligned}$$

$$\boxed{\begin{aligned}
i_p(t) &= \frac{-\omega_p^2 C_p V_0}{\left(1-k^2\right)\left(\omega_+^2 - \omega_-^2\right)} \\
&\quad \times\left\{\frac{\omega_s^2-\omega_+^2}{\omega_+}\sin(\omega_+ t) - \frac{\omega_s^2-\omega_-^2}{\omega_-}\sin(\omega_- t)\right\}. \quad (54)
\end{aligned}}$$

To get the primary and secondary voltages, just integrate the primary and secondary currents:

$$\begin{aligned} v_s(t) &= -\frac{1}{C_s}\int_0^t i_s\, dt' \\ &= -\left(\frac{kNV_0}{1-k^2}\right)\left(\frac{\omega_s^2}{\omega_+^2-\omega_-^2}\right)\left(\cos(\omega_+ t)-\cos(\omega_- t)\right), \end{aligned} \tag{55}$$

$$\begin{aligned} v_p(t) &= V_0 - \frac{1}{C_p}\int_0^t i_p\, dt' \\ &= V_0\left\{1-\left(\frac{1}{1-k^2}\right)\left(\frac{\omega_p^2}{\omega_+^2-\omega_-^2}\right)\right. \\ &\quad \left.\times\left\{\frac{\omega_s^2-\omega_+^2}{\omega_+^2}\left(\cos(\omega_+ t)-1\right)-\frac{\omega_s^2-\omega_-^2}{\omega_-^2}\left(\cos(\omega_- t)-1\right)\right\}\right\}. \end{aligned} \tag{56}$$

Resonance charging is achieved when the circuit parameters describing the circuit are selected so that there is a time $t_0 > 0$ such that energy has been transferred from C_p to C_s and there is no energy stored in the magnetic field of the transformer. These conditions require that

$$i_p(t_0) = 0 \quad \text{and} \tag{57}$$

$$i_s(t_0) = 0. \tag{58}$$

This can occur only if

$$\omega_+ = n\omega_- \quad \text{and} \tag{59}$$

$$\omega_- t_0 = \pi. \tag{60}$$

where n is an integer (since we want v_s to be a maximum at t_0, n must be an even integer). Equation (59) requires that the quantity $1-k^2$ be a function of ω_p, ω_s, and n, given by

$$1-k^2 = \frac{\left(\omega_p^2+\omega_s^2\right)^2}{\omega_p^2\omega_s^2}\frac{n^2}{\left(n^2+1\right)^2}. \tag{61}$$

We derive this relationship by evaluating equation (41) for ω_+ and ω_- and then enforcing equation (59). Substituting equation (61) back into equation (41) gives

$$\omega_+^2 = \frac{\omega_p^2 \omega_s^2}{\omega_p^2 + \omega_s^2} \left(n^2 + 1 \right) \quad \text{and} \tag{62}$$

$$\omega_-^2 = \frac{\omega_p^2 \omega_s^2}{\omega_p^2 + \omega_s^2} \left(\frac{n^2 + 1}{n^2} \right). \tag{63}$$

As an example, figure 3 shows the primary and secondary voltages and currents of a resonant transformer for the conditions $\omega_p = \omega_s$ and $n = 2$. In this case, the voltage gain is N, and there is complete energy transfer between the primary and secondary capacitors.

Figure 3. Normalized voltage and current waveforms in a resonant transformer for $\omega_p = \omega_s$ and $n = 2$.

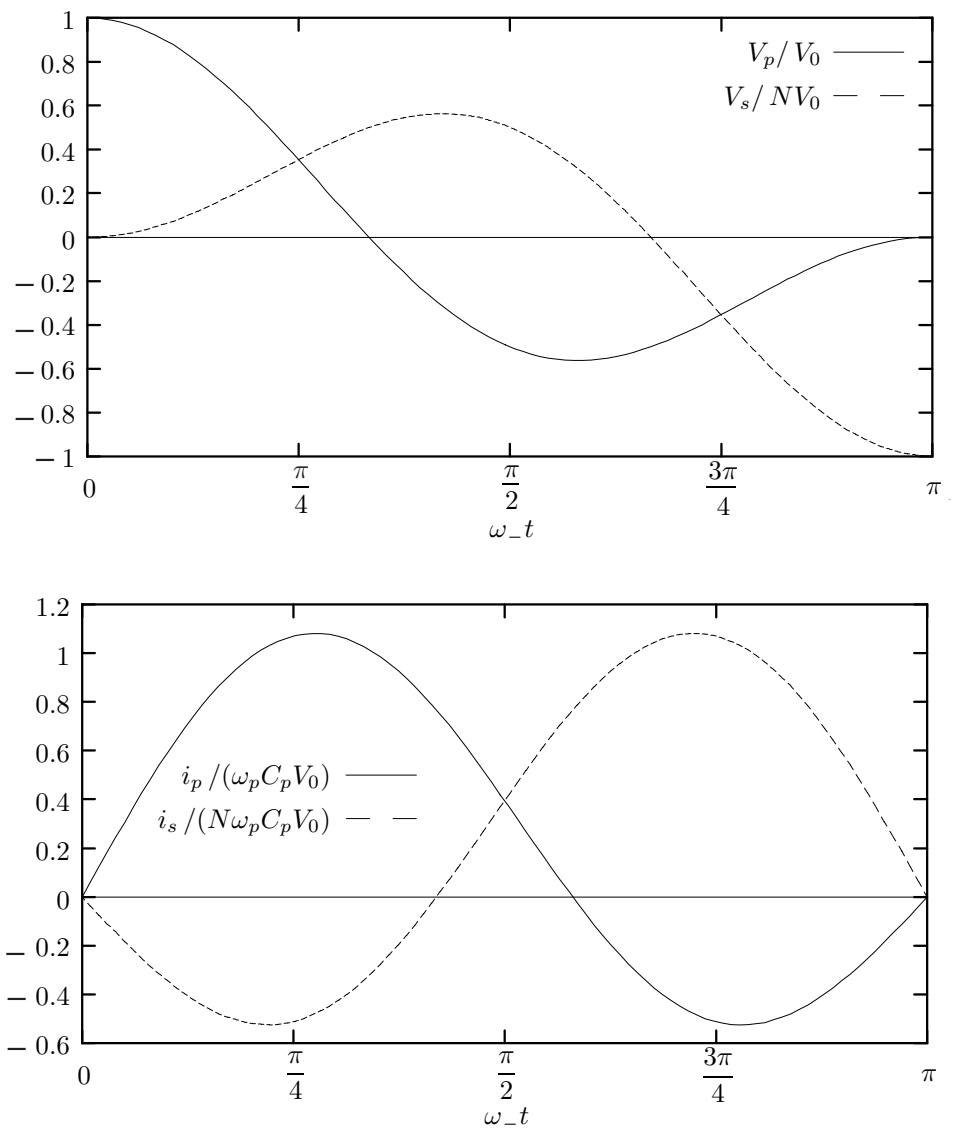

3. Design Methodology for Resonant Charging System

3.1 System Design Parameters

Now that the general solution for the resonant system in figure 2 has been obtained (eq (51), (54), (55), and (56)), we must derive the critical system parameters (those specified at the beginning of the design process) from the resonance equations. In the design process, we specify the capacitance being charged, C_s; the charging voltage $v_s(t_0)$; and the charging voltage V_0 of the primary capacitance C_p. Thus we specify the system voltage gain, given by

$$\begin{aligned} G &= \frac{v_s(t_0)}{V_0} \\ &= -\left(\frac{2kN}{1-k^2}\right)\left(\frac{\omega_s^2}{\omega_+^2-\omega_-^2}\right) \\ &= -2kN\left(\frac{\omega_s^2}{\omega_p^2+\omega_s^2}\right)\left(\frac{n^2+1}{n^2-1}\right). \end{aligned} \tag{64}$$

Note that $|G| < 2N$. In practice, we would usually set $G = N$.

Another system parameter used in the design process is the energy transfer efficiency η, defined by

$$\begin{aligned} \eta &= \left(\frac{1}{2}C_s v_s(t_0)^2\right) \Big/ \left(\frac{1}{2}C_p V_0^2\right) \\ &= 4k^2\left(\frac{\omega_p\omega_s}{\omega_p^2+\omega_s^2}\right)^2\left(\frac{n^2+1}{n^2-1}\right)^2. \end{aligned} \tag{65}$$

This quantity defines the fraction of energy transferred from C_p to C_s during a resonant charging cycle. Squaring equation (64) and dividing it by equation (65) gives the relationship

$$\frac{\omega_s^2}{\omega_p^2} = \frac{1}{\eta}\left(\frac{G}{N}\right)^2 = \delta^2. \tag{66}$$

Thus defining G, N, and η determines the ratio of ω_s to ω_p. The special case of $\omega_p = \omega_s$ deserves special attention, since then

$$\eta = k^2 \left(\frac{n^2+1}{n^2-1}\right)^2 \text{ and} \tag{67}$$

$$k^2 = \left(\frac{n^2-1}{n^2+1}\right)^2. \tag{68}$$

Substituting equation (68) into equation (67) shows that for $\omega_p = \omega_s$ and all n even, $\eta = 1$ and all energy stored in C_p is transferred to C_s. This is not always a desirable condition. If η is significantly less than one, C_p can be used for both filtering and energy storage. The other critical design parameter is usually the maximum value of di_p/dt during the resonant charging cycle. This is because the limiting component in a realistic circuit is the switch that discharges C_p through the primary of the transformer (note that if $\eta < 1$, this would be a partial discharge of C_p):

$$\begin{aligned}
\frac{di_p}{dt} &= -\frac{\omega_p^2 C_p V_0}{(1-k^2)\left(\omega_+^2 - \omega_-^2\right)} \left\{\left(\omega_s^2 - \omega_+^2\right)\cos(\omega_+ t) - \left(\omega_s^2 - \omega_-^2\right)\cos(\omega_- t)\right\} \\
&= -C_p V_0 \frac{\omega_p^2 \omega_s^2}{\left(\omega_p^2 + \omega_s^2\right)^2}\left(\frac{n^2+1}{n^2-1}\right) \\
&\quad \times \left\{\left(\omega_s^2 - n^2\omega_p^2\right)\cos(\omega_+ t) - \left(\omega_s^2 - \frac{\omega_p^2}{n^2}\right)\cos(\omega_- t)\right\} \qquad (69) \\
&= -\omega_p^2 C_p V_0 \frac{\delta^2}{(\delta^2+1)^2}\left(\frac{n^2+1}{n^2-1}\right) \\
&\quad \times \left\{\left(\delta^2 - n^2\right)\cos(\omega_+ t) - \left(\delta^2 - \frac{1}{n^2}\right)\cos(\omega_- t)\right\}. \qquad (70)
\end{aligned}$$

The term di_p/dt will have a maximum magnitude for $t = 0$ if the coefficients of $\cos(\omega_- t)$ and $\cos(\omega_+ t)$ are of opposite sign:

$$\left(\delta^2 - n^2\right)\left(\delta^2 - \frac{1}{n^2}\right) < 0 \tag{71}$$

and

$$\frac{1}{n^2} < \delta^2 < n^2. \tag{72}$$

For this case,

$$\left.\frac{di_p}{dt}\right|_{t=0} = \frac{V_0}{L_p}\frac{\delta^2}{(\delta^2+1)^2}\frac{(n^2+1)^2}{n^2}. \tag{73}$$

The maximum value of $(di_p/dt)|_{t=0}$ determined by the discharge switch specifications δ and the order of the resonance n would now determine the lower limit for the primary inductance L_p of the transformer.

3.2 Design of Dual-Resonance Charging System

One of the major problems we are addressing is the weight of the PFN charging system. If we could use an air-core transformer to step up the voltage, the system weight would be greatly reduced. One requirement for a realizable air-core transformer is that the transformer coupling coefficient k not be too close to one. This requirement led us to consider a dual-resonance charging system.

For dual resonance ($n = 2$, $\omega_p = \omega_s$, $\eta = 1$, and $G = N$), the coupling factor is 0.6 and can be realized in an air-core design. Additionally, the use of an air-core transformer allows for a simpler transformer design process, because analytic methods can be used to calculate and optimize the transformer parameters. For the specific case of dual resonance, the design equations become

$$\omega_+^2 = \frac{5}{2}\omega_p^2, \tag{74}$$

$$\omega_-^2 = \frac{5}{8}\omega_p^2, \tag{75}$$

$$i_p = \frac{\sqrt{10}\omega_p C_p V_0}{8}\left\{2\sin\left(2\omega_- t\right) + \sin\left(\omega_- t\right)\right\}, \tag{76}$$

$$\frac{di_p}{dt} = \frac{5V_0}{16L_p}\left\{4\cos\left(2\omega_- t\right) + \cos\left(\omega_- t\right)\right\}, \tag{77}$$

$$i_s = -\frac{1}{2}\sqrt{\frac{5}{8}}\frac{\omega_p C_p V_0}{N}\left\{2\sin\left(2\omega_- t\right) - \sin\left(\omega_- t\right)\right\}, \tag{78}$$

$$v_p = \frac{V_0}{2}\left\{\cos\left(2\omega_- t\right) + \cos\left(\omega_- t\right)\right\}, \tag{79}$$

$$v_s = -\frac{NV_0}{2}\left\{\cos\left(2\omega_- t\right) - \cos\left(\omega_- t\right)\right\}. \tag{80}$$

If $\mathcal{R}$ is the repetition rate for the charging of capacitor C_s, then the rms currents in the primary and secondary of the transformer are given by

$$\begin{aligned}\langle i_p\rangle_{rms} &= \sqrt{\mathcal{R}\int_0^{\frac{\pi}{\omega_-}} i_p^2\ dt'} \\ &= \sqrt{\frac{25}{32}\sqrt{\frac{2}{5}}\pi C_p V_0\sqrt{\mathcal{R}\omega_p}} \\ &= 1.2459 C_p V_0\sqrt{\mathcal{R}\omega_p} \qquad (81)\end{aligned}$$

and

$$\begin{aligned}\langle i_s\rangle_{rms} &= \sqrt{\mathcal{R}\int_0^{\frac{\pi}{\omega_-}} i_s^2\ dt'} \\ &= \sqrt{\frac{25}{32}\sqrt{\frac{2}{5}}\pi \frac{C_p V_0}{N}\sqrt{\mathcal{R}\omega_p}} \\ &= 1.2459\frac{C_p V_0}{N}\sqrt{\mathcal{R}\omega_p} \\ &= \frac{\langle i_p\rangle_{rms}}{N}. \qquad (82)\end{aligned}$$

The maximum of i_p occurs where $di_p/dt = 0$. Let $\phi = \omega_- t$; then the necessary conditions for the maximum are

$$\begin{aligned}4\cos(2\phi) + \cos(\phi) &= 0, \\ 8\cos^2(\phi) + \cos(\phi) - 4 &= 0, \qquad (83)\end{aligned}$$

or

$$\begin{aligned}\cos(\phi) &= 0.647364, -0.772364, \\ \phi &= 49.6569^\circ, 140.567^\circ, \\ 2\sin(2\phi) + \sin(\phi) &= 2.7358, -1.32718, \qquad (84) \\ \max\{i_p\} &= 1.081428\omega_p C_p V_0. \qquad (85)\end{aligned}$$

The result of this procedure for the secondary is

$$\max\{i_s\} = 1.081428\frac{\omega_p C_p V_0}{N}. \qquad (86)$$

Since the case of dual-resonance charging satisfies equation (72), the maximum value for di_p/dt is

$$\max\left\{\frac{di_p}{dt}\right\} = \frac{25V_0}{16L_p}. \qquad (87)$$

Since there is no reverse-conducting solid-state switch in the secondary circuit, we are not concerned with the value of di_s/dt.

4. Example of Modulator Charging System Design

4.1 System Definition

Figure 4 shows the circuit of a complete rf tube modulator system. In this circuit, the PFN is charged to $\max\{v_s\} = 42$ kV and $\mathcal{E}_s = 250$ J, at a maximum repetition rate of $\mathcal{R} = 300$ Hz. The prime power for the system consists of a generator, phase controller, and rectifier that can charge an energy storage capacitor C_f to a voltage of $V_0 = 550$ Vdc. To totally define the system, we need to specify the ratio of energy stored in C_f to be transferred to C_p, the time T_{fp} for the energy to transfer from C_f to C_p, and the time T_{ps} for the energy to transfer from C_p to C_s (the total capacitance of the PFN). Note that the sum of the transfer times must be less than the reciprocal of the repetition rate. Table 1 shows the parameters that we use to define our system.

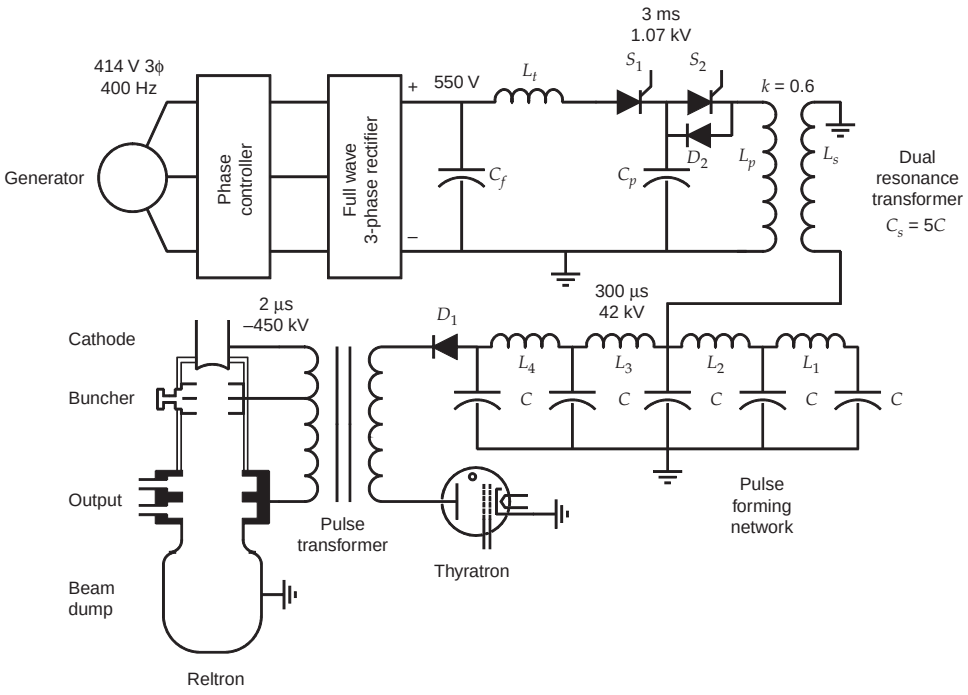

Figure 4. Reltron modulator.

Table 1. Design parameters for PFN charging system.

Parameter	Value
$\max\{v_s\}$	42 kV
$\mathcal{E}_s$	250 J
$\mathcal{R}$	300 Hz
$\frac{\mathcal{E}_f}{\mathcal{E}_s}$	10
V_0	550 V
T_{fp}	3 ms
T_{ps}	0.3 ms

4.2 Circuit Design

Using the equations in sections 2.1 and 3.1 of this report, one can obtain the derived circuit parameters shown in table 2. The voltage and current waveforms for this set of design parameters are shown in figure 5. The issues to be addressed in the realization of this circuit follow:

1. Are there commercially available thyristors and diodes for S_1, S_2, D_1, and D_2 in figure 4 that can meet the specifications in table 2?

Table 2. Derived circuit parameters for PFN charging system with rectified supply voltage of 550 V.

Component	Parameter	Value
Transfer inductor	C_f	16.5 mF
	L_t	2.2 mH
	$\max\{i_t\}$	238 A
	$\langle i_t \rangle_{rms}$	160 A
	$\max\{di_t/dt\}$	0.25 A/μs
Transformer primary	$\max\{v_p\}$	1.07 kV
	C_p	424 μF
	L_p	13.44 μH
	$\max\{i_p\}$	6.5 kA
	$\langle i_p \rangle_{rms}$	1.13 kA
	$\max\{di_p/dt\}$	125 A/μs
Transformer secondary	C_s	283 nF
	L_s	20.61 mH
	$\langle i_s \rangle_{rms}$	29 A
	$\max\{i_s\}$	166 A

Figure 5. Voltage and current waveforms for dual resonance charging.

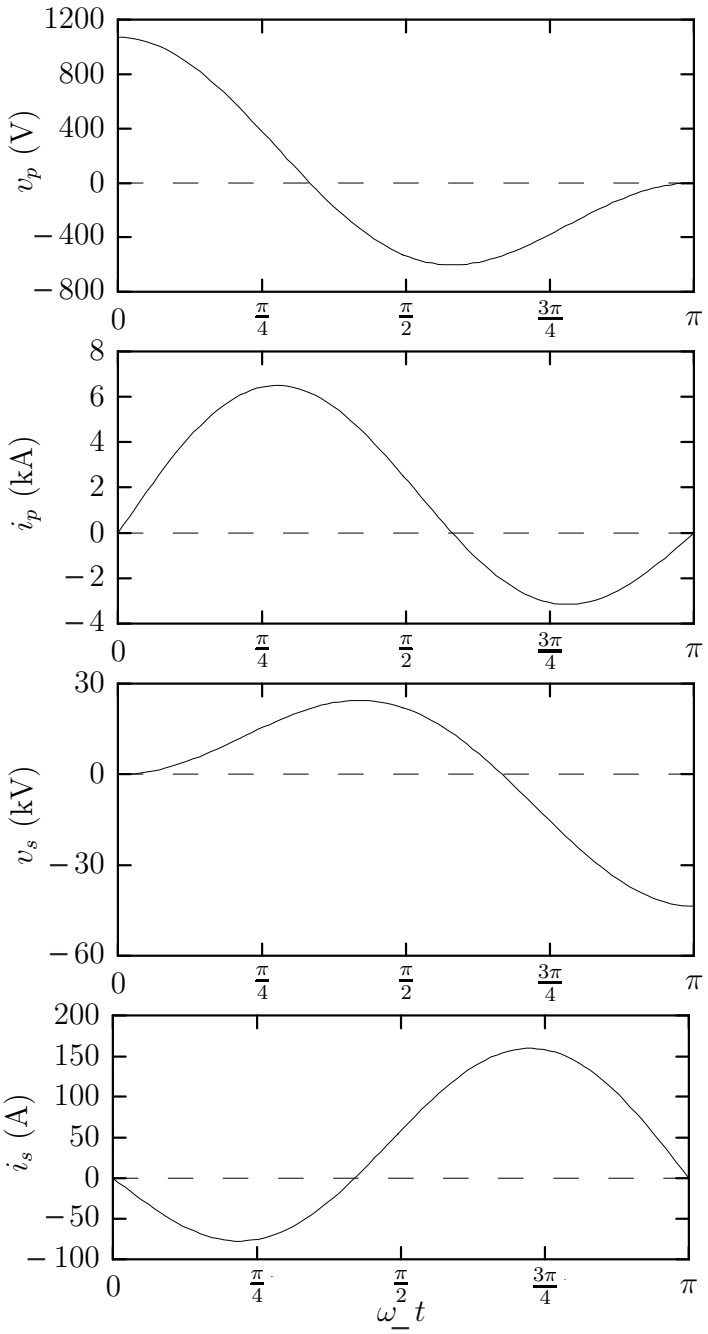

2. Can the transfer inductor and dual-resonance transformer be made small enough to be comparable to the size of the rest of the modulator?
3. Will the losses in the inductor and transformer substantially degrade the performance of the system?
4. What are the size and cost of the filter capacitor C_f and primary capacitor C_p?
5. Will the losses in the capacitors substantially degrade the performance of the system?

4.3 Selection of Solid-State Switches

The only solid-state component that could present a difficulty in terms of commercial-off-the-self (COTS) availability is the thyristor switch on the primary side of the dual-resonance transformer (S_2 in fig. 4). The requirements for this component are shown in table 2. In a search of the manufacturing literature, we found a high-speed thyristor produced by the Silicon Power Corporation (SPCO) that satisfied these requirements. The device characteristics relevant to our application are shown in table 3.

The device characteristics shown in table 3 are adequate for our switching requirements. Note that if the voltage on the primary capacitor of the dual-resonance circuit can be increased (by a higher voltage generator, perhaps), the peak di/dt and peak current requirements would both decrease.

Table 3. Device parameters for SPCO C712PE high-speed 53-mm silicon-controlled rectifier.

Parameter	Value
Forward voltage (V_{DRM}) and Reverse voltage (V_{RRM}), repetitive, junction temperature $T_J = -40$ to $+125$ °C	1500 V
Transient peak reverse voltage, V_{RSM}, $T_J = -40$ to $+125$ °C	1600 V
Repetitive di/dt rating	200 A/μs
Peak forward current for 300-μs pulse, 300-Hz repetition rate	>7 kA

4.4 Selection of Energy Storage Capacitors

Two capacitors (table 1) are required for the resonant charging power supply design. The specifications for these capacitors are shown in table 4.

Table 4. Capacitor parameters for dual-resonance charging system.

Capacitor type	Capacitance	Charging voltage	Voltage reversal	RMS current	Charging time
Filter	16.5 mF	550 V	0%	160 A	300 ms
Dual resonance	424 μF	1.07 kV	50%	1.13 kA	300 μs

The filter capacitors can use electrolytics in what is essentially the role of a filter capacitor (10-percent energy discharge, 5-percent voltage discharge maximum per pulse at a maximum repetition rate of 300 Hz). The problem with using electrolytics is that the highest standard voltage rating on a high-capacity electrolytic capacitor that we could find was 450 Vdc (for Mallory aluminum electrolytic CGH772T450X5L), with a capacitance of 7.7 mF and a size of 3 in. deep $\times\ 8\frac{5}{8}$ in. long. In a series parallel arrangement, eight capacitors would be required to come close enough to the required capacitance for a practical design. The size of the eight-capacitor package would be approximately $6 \times 6 \times 18$ in. If the rectified output voltage of the prime power system can be increased by a factor of two, we avoid the need for an electrolytic capacitor and inductor before the input to the dual-resonance transformer.

The capacitor for the primary of the dual-resonance transformer has more stringent requirements (table 4), because of the voltage reversal (see fig. 5) and high rms current. In searching the specification literature of the Condenser Products Corporation, we found two capacitors in their KMOC series that we could interpolate to our requirements. The specifications of these capacitors are as follows:

Part No.	Voltage rating (kV)	Capacitance (μF)	Dimensions, $D \times W \times H$ (in.)	Energy density (kJ/m^3)
1M500	1	500	$5\frac{1}{4} \times 13\frac{1}{2} \times 12$	18.3
3M400	3	400	$6 \times 18 \times 28$	36.6

Since the value of the capacitor used in the dual-resonance charging circuit is fairly critical, a custom-made capacitor is required. To bound the size of this capacitor, we considered the characteristics of the 1M500 and 3M400 models. Extrapolating from the 3M400, we would expect that the size (linear dimensions) of a capacitor with an energy density of 424 μF/3 kV would be 2 percent greater than that of the 3M400. This would be a worst-case analysis, since even for a 50-percent voltage reversal, we would not require a capacitor rated at three times the charging voltage. The implications of higher voltage operation are also favorable for the primary dual-resonance capacitor. If the

rectified output of the prime power supply could charge the primary dual-resonance capacitor to 2.14 kV, the required capacitance would be reduced to 106 μF. The closest 3-kV capacitor to this value is the 3M100ES, at a capacitance of 100 μF and a size in inches of $5\frac{1}{4}D \times 13\frac{1}{2}W \times 10\frac{1}{2}H$. Additionally, raising the charging voltage by a factor of 2 would reduce the rms current in the capacitor by a factor of 2.

4.5 Design of Air-Core Inductors

The self-inductances of an infinitely thin cylindrical current sheet can be calculated [3, p 31]. For a coil of length l (in centimeters), radius a (in centimeters), and number of turns N, the inductance L (in henries) is

$$L = \frac{4\pi \times 10^{-9} N^2}{3} \sqrt{l^2 + 4a^2} \left\{ K - E + \frac{4a^2}{l^2} (E - k) \right\}, \tag{88}$$

where

$$k = \frac{2a}{\sqrt{l^2 + 4a^2}} \tag{89}$$

is the modulus of K and E, the complete elliptic integrals of the first and second kinds.

The k used in this section refers to the modulus of the elliptic integrals and not the transformer coupling coefficient (as in sect. 2). While this could be confusing, the use of k for the elliptic integral modulus is so universal that it would be difficult for the reader to compare the inductance formulas in this report with the formulas for elliptic integrals in the standard references [4, p 8]. Also, we are using centimeters in all our formulas because the primary reference [3] uses centimeters (cgs units); being consistent with the primary reference will reduce the likelihood of confusion for anyone who wishes to consult that reference. The only allowance we make is that our inductances are in henries and not in cgs units (multiply the inductance in cgs units by 10^{-9} to get henries).

For two coaxially concentric, infinitely thin current sheets with radii a_1 and a_2, lengths l_1 and l_2, and turns N_1 and N_2 (see fig. 6), the mutual inductance between the winding is given by

$$M_{12} = \frac{4\pi \times 10^{-9} N_1 N_2}{l_1 l_2} \left\{ w\left(\frac{l_2 + l_1}{2}\right) - w\left(\frac{l_2 - l_1}{2}\right) \right\}, \tag{90}$$

Figure 6. Coil parameters for calculation of mutual inductance.

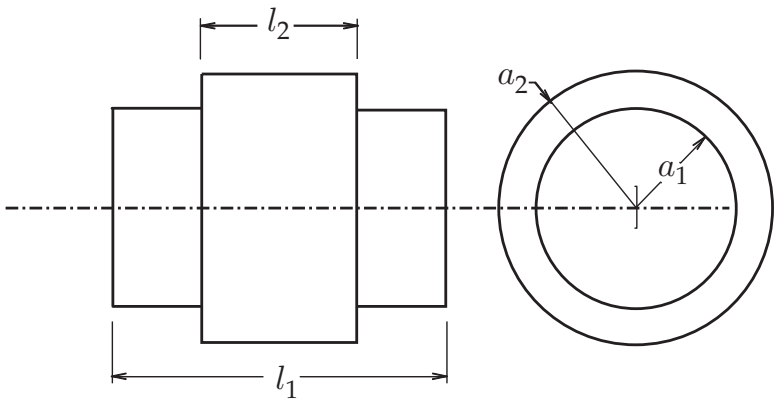

where the function $w(x)$ is defined by

$$w(x) = \frac{2x^2\sqrt{a_1 a_2}}{k}(K-E) + \frac{8(a_1 a_2)^{\frac{3}{2}}}{3k}\left\{K - \left(\frac{2}{k^2}-1\right)(K-E)\right\} + |x|\left|a_1^2 - a_2^2\right|\left\{KE(\theta,k') - (K-E)F(\theta,k') - \frac{\pi}{2}\right\}. \quad (91)$$

The modulus k, complementary modulus k', and angle θ for the complete (K and E) and incomplete ($E(\theta,k')$ and $F(\theta,k')$) elliptic integrals in equation (91) are defined by

$$k = \sqrt{\frac{4a_1 a_2}{x^2 + (a_1 + a2)^2}}, \quad (92)$$

$$k' = \sqrt{1-k^2}, \quad \text{and} \quad (93)$$

$$\sin\theta = \sqrt{\frac{1+\left(\frac{x}{a_1+a_2}\right)^2}{1+\left(\frac{x}{a_1-a_2}\right)^2}}, \quad 0<\theta<\frac{\pi}{2}. \quad (94)$$

Note that when K and E are referred to without an argument, they are always to be taken as the complete elliptic integrals with modulus k. In equation (91), the incomplete elliptic integrals $E(\theta,k')$ and $F(\theta,k')$ are to be evaluated at the angle θ given in equation (94) and at modulus k' given by equation (93) (use the complement of the modulus of the complete elliptic integrals as the modulus of the incomplete elliptic integrals).

For a multilayer inductor, one can calculate the total inductance by applying equation (88) to each layer to calculate the inductance L_i of the single layer,

and equation (90) to calculate the mutual inductance M_{ij} between each pair of layers. The total inductance of the series-connected layers N_l is then

$$L = \sum_{i=1}^{N_l} \left\{ L_i + 2 \sum_{j=i+1}^{N_l} M_{ij} \right\}. \tag{95}$$

For two coils with multiple layers (the layers series connected in each coil), the mutual inductance between the two coils (designated with the subscripts p and s for primary and secondary) is given by

$$M = \sum_{i=1}^{N_{pl}} \sum_{j=1}^{N_{sl}} M_{p_i s_j}. \tag{96}$$

(We designate the mutual inductance between the i^{th} layer of coil p and the j^{th} layer of coil s as $M_{p_i s_j}$.) The design of the inductor starts with the parameters generated from the circuit model. The critical parameters are the inductance L, the rms current $\langle i \rangle_{rms}$, and the maximum voltage across the coil, $\max\{v\}$. The value of $\langle i \rangle_{rms}$ determines the minimum wire size that can be used, which in turn determines the number of turns per unit length in a layer, dN_s/dl, and the minimum thickness of the layer, $\{dN_s/dl\}^{-1}$. Thus if we specify the number of turns per layer and the number of layers in the coil, we are also specifying the length and thickness of the coil. At this point we know L and dN/dl and can pick the number of layers in the coil, which we can then vary to minimize the size and power dissipation in the coil. From experience, we say that the coil volume $\pi a^2 l$ will be minimized if $l = 2a$ (we are letting a be the mean radius of the coil). Under these restrictions, the only unknown in equation (95) is l, which one can determine by solving equation (95) with a simple bracketing and bisection algorithm [5, p 353]. The maximum voltage across the inductor affects the design of how the windings are physically configured. As an example of the design procedure, we present the design of the inductor L_t.

The inductor L_t operates at an rms current of 160 A. This current requires a wire size of at least 00 AWG. The maximum voltage across L_t is no greater than 550 V. Since providing 550 V of insulation between winding layers is easily done, a simple multilayer coil is acceptable in order to minimize the size of the inductor. If we evaluate equation (88) to determine the size of coils containing 1 through 6 layers, we have the results in table 5. In table 5, the average power dissipated in the coil is $R \langle i \rangle_{rms}^2$, where R is the resistance of the inductor. Since the minimum power dissipation (for our ratio of $l/a = 2$)

Table 5. Inductor ($L_t = 2.2$ mH) dimensions as a function of number of winding layers for 00 AWG wire.

Layers	Length (cm)	Radius (cm)	Thickness (cm)	Power (W)
1	64.9	32.8	0.92	943
2	41.7	21.0	1.85	775
3	31.5	16.0	2.78	669
4	25.9	13.2	3.70	606
5	23.1	12.1	4.63	622
6	24.1	13.5	5.56	864

occurs for $N_l = 4$ and the coil is of reasonable size, we select four layers. Note that the skin effect should not significantly affect our calculation, since the ring frequency of the circuit is 167 Hz; using this frequency yields a skin depth of 0.51 cm in Cu, while the 00 AWG wire has a radius (including insulation) of 0.46 cm.

4.6 Design of Air-Core Transformer

The first step in designing the air-core transformer is to design the secondary winding. Proceeding in the same manner as with the transfer inductor, we know the required inductance and rms current capacity (see table 2). Table 6 shows the results of this calculation as a function of coil layers.

The main problem to solve in the design of the transformer secondary is that it must withstand a much greater peak voltage (42 kV) than the transfer inductor (550 V). The simplest solution would be to use a single-layer winding to provide continuous voltage grading. If the size of the single-layer coil in table 6 is acceptable from a system standpoint, this would be the best solution. If the single-layer coil is too large, we then require a coil with an odd number of layers so that we can configure the secondary of the transformer as several smaller coils connected in series, as shown in figure 7.

An odd number of layers is required so that the input and output of each section are at the opposite ends of each section. The secondary winding would then consist of several smaller coils wired in series. This series configuration is used so that the interlayer insulation requirements of each individual coil are kept low. The interlayer insulation requirement determines how many axial coil sections are required. In the case shown in figure 7 (three layers and three sections), if a total voltage capability of 45 kV is needed, the interlayer insulation requirement would be 5 kV, with an inter-section in-

Table 6. Transformer dimensions as a function of number of winding layers for 11 AWG wire, assuming zero stray inductance in primary circuit ($k = 0.6$) and a 0.5-cm-thick primary winding.

No. of layers	Secondary				Insulation (cm)	Primary				Total power dissip. (W)
	Turns	Length (cm)	Radius (cm)	Power dissip. (W)		Turns	Length (cm)	Radius (cm)	Power dissip. (W)	
1	236	54.4	27.2	1388	5.51	6	28.8	21.3	738	2126
2	298	34.3	17.3	1112	3.29	8	22.0	13.5	1084	2196
3	339	26.0	13.2	968	2.19	9	16.4	10.4	1423	2391
4	376	21.7	10.8	878	1.51	10	13.8	8.6	1714	2592
5	400	18.4	9.4	817	0.98	10	10.2	7.6	2063	2880
6	432	16.6	8.5	606	0.80	11	10.1	6.8	2232	2838

Figure 7. Multilayer, multisection coil for grading of high voltage.

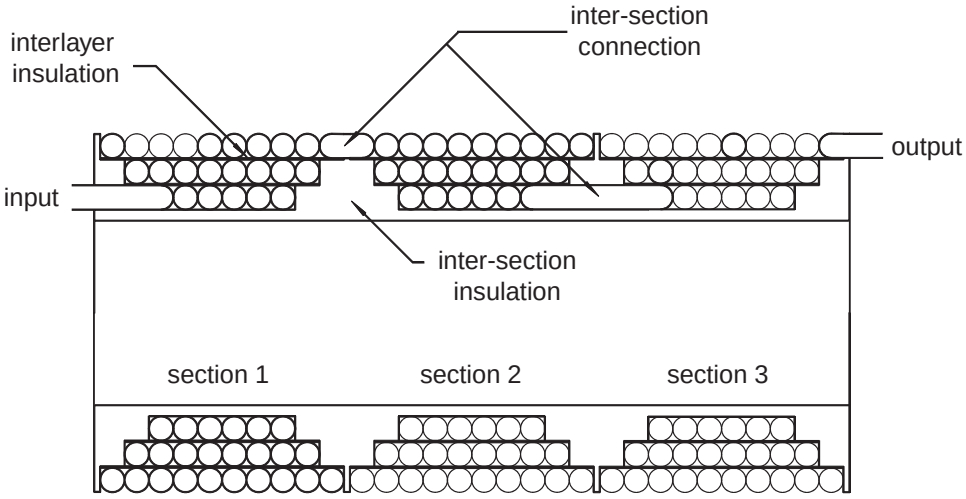

sulation of 20 kV (since the insulation between sections can be made much thicker than the insulation between layers, this configuration is not difficult to achieve).

Once the dimensions of the secondary are calculated, the primary must be designed. For the primary, there is much less freedom of choice, since not only must the primary winding have a specified inductance, it must also be dimensioned to provide a given coupling coefficient k. If there are no significant stray inductances in the primary or secondary circuits of the dual-resonance system, then we require $k = 0.6$. If the stray inductances are a significant fraction of the inductances of the primary winding or the secondary winding, the transformer will have to be designed with a lower primary and/or secondary inductance and a higher coupling coefficient. In

practice, the stray inductance is usually only significant on the primary side of the transformer. If L_{stray} is the stray inductance on the primary side, if L_p is the required sum of the stray inductance, and if the system coupling coefficient is 0.6, then the actual primary inductance of the transformer is $L_p - L_{stray}$, and the required k of the transformer is

$$k = 0.6\sqrt{\frac{L_p}{L_p - L_{stray}}}. \tag{97}$$

The starting point for the design of the primary is an estimate of the number of turns that are allowed. Because of the constraints on both k and L_p, the allowed values of N_p are limited. To start, we assume that both the primary and secondary windings have the same length and mean radius and calculate the inductance of a one-turn coil with these dimensions. If that inductance is denoted as L_{p_0}, then the number of turns is $N_p = \sqrt{L_p/L_{p_0}}$. In general, the value of N_p calculated will not be an integer. The value used in our calculation is the near-integer value to N_p. We should consider the value of N_p so selected the starting point of our design optimization.

Table 6 shows the results of such a transformer design for zero stray primary inductance. The "insulation" column is the distance between the inner radius of the primary and the outer radius of the secondary. The insulation in this gap must be able to hold off the charging voltage on C_s (in our case 42 kV). We can use a secondary with one, three, or five layers so that the coil design shown in figure 7 can be implemented (three or five layers). Assuming that the insulation between the primary and secondary is sufficient, the major difference between the designs for different layer numbers is the volume of the transformer and the power dissipated in the windings. The total power dissipation for a transformer with five-layer secondary is 34 percent greater than the dissipation in a transformer with a one-layer secondary. The five-layer transformer is 34 percent of the length and 31 percent of the radius of a one-layer transformer. Note that the skin effect in the secondary winding should not be significant, since at 3.33 kHz (high frequency of dual resonance) the skin depth is 0.11 cm, while the radius of 11 AWG wire (including insulation) is 0.11 cm. The thickness of the primary winding is 0.5 cm. For a spiral-tape-wound six-turn primary, the tape thickness would be 0.083 cm (≈3 mil Cu tape), and the skin effect would not be a problem. Note that the primary of the transformer is inside the secondary. This configuration indicates that in order to reduce stray inductances and minimize magnetic field perturbations, the primary winding should be connected axially with a parallel-plate feed system.

Table 7 shows the design of a transformer with 2 μH of stray inductance on the primary side. The only significant difference between this design and the design in table 6 is that there is less power dissipation in the primary because there is less inductance, and hence less resistance in the primary winding. (Note that if a trimming inductor is needed in the primary circuit, it will have some fraction of the power dissipation difference between tables 6 and 7.)

Table 7. Transformer dimensions as a function of number of layers in secondary for 11 AWG wire, assuming 2 μH stray inductance in primary circuit ($k = 0.65$) and a 0.5-cm-thick primary winding.

No. of layers	Secondary				Insulation (cm)	Primary				Total power dissip. (W)
	Turns	Length (cm)	Radius (cm)	Power dissip. (W)		Turns	Length (cm)	Radius (cm)	Power dissip. (W)	
1	236	54.4	27.2	1388	5.32	6	38.1	21.5	562	1950
2	298	34.3	17.3	1112	2.66	7	20.9	14.1	914	2026
3	339	26.0	13.2	968	1.75	8	16.2	10.9	1185	2153
4	376	21.7	10.8	878	1.19	9	14.1	8.9	1415	2293
5	400	18.4	9.4	817	0.68	9	10.4	7.9	1703	2520
6	432	16.6	8.5	606	0.57	10	10.6	7.0	1830	2436

5. Conclusions

The design as shown in figure 4, in which the prime power system provides a 550-V rectified output, is feasible. Significant improvements, however, can be made if we increase the rectified output voltage of the prime power system. The most difficult aspect of the system design is the power dissipation in the primary of the dual-resonance transformer and in the primary dual-resonance energy-storage capacitors, because of the very high rms currents in these parts of the circuit. A lesser problem is uniform excitation of the primary of the dual resonance transformer. Because the primary winding has so few turns (six), care must be taken to ensure that there is no significant variation of current density along the axial cross section of the tape winding. The tape winding is required to minimize the inductance of the connection to the primary winding and to ensure that skin-depth effects will be minimized.

References

1. G. N. Glasoe and J. V. Lebacqz. *Pulse Generators*. Dover Publications, Inc., New York, 1965.

2. M. Abramowitz and I. A. Stegun. *Handbook of Mathematical Functions*. Dover Publications, Inc., New York, 1972.

3. C. Snow. *Formulas for Computing Capacitance and Inductance*. National Bureau of Standards Circular 544, U.S. Government Printing Office, Washington, DC, 1954.

4. P. F. Byrd and M. D. Friedman. *Handbook of Elliptic Integrals for Engineers and Physicists*. Springer-Verlag, Berlin, Germany, 1954.

5. W. H. Press, S. A. Teukolsky, W. T. Vetterling, and B. P. Flannery. *Numerical Recipes in C, The Art of Scientific Computing*. Cambridge University Press, New York, 1994.

Distribution

Admnstr
Defns Techl Info Ctr
Attn DTIC-OCP
8725 John J Kingman Rd Ste 0944
FT Belvoir VA 22060-6218

Defns Threat Reduction Agcy
Attn DTRA/ESE D Devany
6801 Telegraph Rd
Alexandria VA 22310-3398

Ofc of the Dir Rsrch and Engrg
Attn R Menz
Pentagon Rm 3E1089
Washington DC 20301-3080

Ofc of the Secy of Defns
Attn ODDRE (R&AT)
Attn ODDRE (R&AT) S Gontarek
The Pentagon
Washington DC 20301-3080

OSD
Attn OUSD(A&T)/ODDDR&E(R) R J Trew
Washington DC 20301-7100

AMCOM MRDEC
Attn AMSMI-RD W C McCorkle
Redstone Arsenal AL 35898-5240

CECOM
Attn PM GPS COL S Young
FT Monmouth NJ 07703

DARPA
Attn M Freeman
3701 N Fairfax Dr
Arlington VA 22203-1714

Dir for MANPRINT
Ofc of the Deputy Chief of Staff for Prsnnl
Attn J Hiller
The Pentagon Rm 2C733
Washington DC 20301-0300

Hdqtrs Dept of the Army
Attn DAMO-FDT D Schmidt
400 Army Pentagon Rm 3C514
Washington DC 20301-0460

TACOM Rsrch, Dev, & Engrg Ctr
Attn D DiCesare
Attn G Kahlil
Attn T Burke
PO Box 249
Warren MI 48090-0249

US Army Armament Rsrch Dev & Engrg Ctr
Attn AMSTA-AR-TD M Fisette
Bldg 1
Picatinny Arsenal NJ 07806-5000

US Army Belvoir RD&E Ctr
Attn SATBE-FGE J Ferrick
FT Belvoir VA 22060

US Army CECOM RDEC
Attn AMSEL-RD-IW-A D Helm
Attn AMSEL-RD-NV-OD R Irwin
Attn J Swartz
Bldg 2705
FT Monmouth NJ 07703-5206

US Army CECOM
RDEC Intllgnc & Info Warfare Dirctrt
Attn AMSEL-RD-IE-DS-EC R Troisio
Bldg 2705
FT Monmouth NJ 07703-5211

US Army Commctn-Electronics Cmnd
Night Vision & Electronic Sensors Dirctrt
Attn AMSEL-RD-NV-CD-MN S Schaedel
10221 Burbeck Rd Ste 430
FT Belvoir VA 22060-5806

US Army Edgewood RDEC
Attn SCBRD-TD G Resnick
Aberdeen Proving Ground MD 21010-5423

US Army Info Sys Engrg Cmnd
Attn ASQB-OTD F Jenia
FT Huachuca AZ 85613-5300

US Army Natick RDEC Acting Techl Dir
Attn SSCNC-T P Brandler
Natick MA 01760-5002

Distribution (cont'd)

Director
US Army Rsrch Ofc
4300 S Miami Blvd
Research Triangle Park NC 27709

US Army Simulation, Train, & Instrmntn Cmnd
Attn J Stahl
12350 Research Parkway
Orlando FL 32826-3726

US Army Tank-Automtv Cmnd Rsrch, Dev, & Engrg Ctr
Attn AMSTA-TA J Chapin
Warren MI 48397-5000

US Army Train & Doctrine Cmnd
Battle Lab Integration & Techl Dirctrt
Attn ATCD-B J A Klevecz
FT Monroe VA 23651-5850

US Military Academy
Mathematical Sci Ctr of Excellence
Attn MDN-A MAJ M D Phillips
Dept of Mathematical Sci Thayer Hall
West Point NY 10996-1786

Cmnd Ofcr Nav Rsrch Lab
Attn Code 6843 D Abe
4555 Overlook Ave SW
Washington DC 20375-5320

Nav Surface Warfare Ctr
Attn Code B07 J Pennella
17320 Dahlgren Rd Bldg 1470 Rm 1101
Dahlgren VA 22448-5100

US Air Force Phillips Lab
Attn J O'Loughlin
Attn K Hackett
3550 Aberdeen Ave SE
Kirtland Air Force Base NM 87112-5776

DARPA
Attn B Kaspar
3701 N Fairfax Dr
Arlington VA 22203-1714

Hicks & Associates, Inc
Attn G Singley III
1710 Goodrich Dr Ste 1300
McLean VA 22102

Mission Rsrch Corp
Attn M Bollen
8560 Cinderbed Rd Ste700
Newington VA 22122

Mission Rsrch Corp
Attn J Havey
1720 Randolph Rd SE
Albuquerque NM 87106-4245

NorthStar Rsrch
Attn R Richter-Sand
4421 A McLeod NE
Albuquerque NM 87109

Palisades Inst for Rsrch Svc Inc
Attn E Carr
1745 Jefferson Davis Hwy Ste 500
Arlington VA 22202-3402

System Planning Corp
Attn D Wiedenhiemer
1429 North Quincy Street
Arlington VA 22207

US Army Rsrch Lab
Attn AMSRL-CI-LL Techl Lib (3 copies)
Attn AMSRL-CS-AS Mail & Records Mgmt
Attn AMSRL-CS-EA-TP Techl Pub (3 copies)
Attn AMSRL-SE-D E Scannell
Attn AMSRL-SE-DP A Bromborsky (12 copies)
Attn AMSRL-SE-DP R A Kehs
Attn AMSRL-SE-DP T F Podlesak (12 copies)
Attn AMSRL-SE-DS L Jasper
Attn AMSRL-SE-DS W O Coburn
Attn AMSRL-WT-NF M Berry
Adelphi MD 20783-1197

REPORT DOCUMENTATION PAGE

Form Approved
OMB No. 0704-0188

1. AGENCY USE ONLY *(Leave blank)*	2. REPORT DATE	3. REPORT TYPE AND DATES COVERED
	December 1998	Final, October 1997 to May 1998

4. TITLE AND SUBTITLE Analysis and Design of Resonant Charging System

5. FUNDING NUMBERS

DA PR: A140
PE: 62120A

6. AUTHOR(S) Alan Bromborsky and Thomas Podlesak

7. PERFORMING ORGANIZATION NAME(S) AND ADDRESS(ES)
U.S. Army Research Laboratory
Attn: AMSRL-SE-DP email: brombo@arl.mil
2800 Powder Mill Road
Adelphi, MD 20783-1197

8. PERFORMING ORGANIZATION REPORT NUMBER
ARL-TR-1819

9. SPONSORING/MONITORING AGENCY NAME(S) AND ADDRESS(ES)
U.S. Army Research Laboratory
2800 Powder Mill Road
Adelphi, MD 20783-1197

10. SPONSORING/MONITORING AGENCY REPORT NUMBER

11. SUPPLEMENTARY NOTES
ARL PR: 8NEYXX
AMS code: 622120.140

12a. DISTRIBUTION/AVAILABILITY STATEMENT Approved for public release; distribution unlimited.

12b. DISTRIBUTION CODE

13. ABSTRACT *(Maximum 200 words)*

The circuit equations are constructed and solved for a simple resonant (single-pole) circuit and a dual-resonance (double-pole) capacitor charging system. Design equations are derived from the solutions. As an example, a command charging system for a capacitor is designed, with detailed equations given for the inductor and transformer analysis; an evaluation of suitable commercially available thyristors and capacitors is also provided.

14. SUBJECT TERMS
Resonant dual charging

15. NUMBER OF PAGES
41

16. PRICE CODE

17. SECURITY CLASSIFICATION OF REPORT	18. SECURITY CLASSIFICATION OF THIS PAGE	19. SECURITY CLASSIFICATION OF ABSTRACT	20. LIMITATION OF ABSTRACT
Unclassified	Unclassified	Unclassified	SAR

NSN 7540-01-280-5500

Standard Form 298 (Rev. 2-89)
Prescribed by ANSI Std. Z39-18
298-102

DEPARTMENT OF THE ARMY
U.S. Army Research Laboratory
2800 Powder Mill Road
Adelphi, MD 20783-1197